



Contents lists available at SciVerse ScienceDirect

Physica B

journal homepage: www.elsevier.com/locate/physb

Sensitizing effects of ZnO quantum dots on red-emitting Pr³⁺-doped SiO₂ phosphor

P.S. Mbule^a, G.H. Mhlongo^{a,b}, Shreyas S. Pitale^a, H.C. Swart^a, O.M. Ntwaeaborwa^{a,*}

^a Department of Physics, University of the Free State, Bloemfontein ZA9300, South Africa

^b National Centre for Nanostructure Materials, Centre for Scientific and Industrial Research, Pretoria ZA0001, South Africa

ARTICLE INFO

Keywords:
Quantum dots
Phosphor
Absorption
Cathodoluminescence

ABSTRACT

In this study, red cathodoluminescence (CL) ($\lambda_{\text{emission}}=614$ nm) was observed from Pr³⁺ ions in a glassy (amorphous) SiO₂ host. This emission was enhanced considerably when ZnO quantum dots (QDs) were incorporated in the SiO₂:Pr³⁺ suggesting that the ZnO QDs transferred excitation energy to Pr³⁺ ions. That is, ZnO QDs acted to sensitize the Pr³⁺ emission. The sol-gel method was used to prepare ZnO-SiO₂:Pr³⁺ phosphors with different molar ratios of Zn to Si. The effects of the ZnO QDs concentration and the possible mechanisms of energy transfer from ZnO to Pr³⁺ are discussed. In addition, the electronic states and the chemical composition of the ZnO-SiO₂:Pr³⁺ phosphors were analyzed using X-ray photoelectron spectroscopy (XPS).

© 2011 Elsevier B.V. All rights reserved.

1. Introduction

ZnO is a semiconductor with a bulk wide band gap (~3.29–3.37 eV) and has been a subject of intense research interest lately. It is the most widely studied semiconducting oxide at the nanoscale with attractive features for applications in lighting [1,2]. It is well known that the ZnO QDs with particle sizes ranging from 3 to 10 nm exhibit dual emission in the UV (~372 nm) and the visible (~510–580 nm) regions associated, respectively, with excitonic recombination and defect states. Recent studies have demonstrated that when the ZnO QDs were incorporated in rare-earth-activated SiO₂ [3–8], defects emission of the ZnO QDs was suppressed and emission from the rare-earths increased considerably. In this study, the sensitizing effects of ZnO QDs in the sol-gel ZnO-SiO₂:Pr³⁺ phosphor were evaluated.

2. Experimental

SiO₂ doped with Pr³⁺ was prepared by hydrolyzing tetraethylorthosilicate (TEOS) with a solution of H₂O, ethanol and dilute nitric acid. The mixture was stirred for 1 h at room temperature, and a desired amount of Pr(NO₃)₃·6H₂O dissolved in ethanol was added to the solution and stirred for another 30 min. ZnO QDs were prepared by dissolving anhydrous zinc acetate (Zn(CH₃COO)₂) in boiling ethanol and the resulting solution was

cooled in ice and then combined with the ethanol solution of sodium hydroxide (NaOH) in ice water. The unwanted CH₃COO⁻ and Na⁺ impurities were removed by centrifuging and washing repeatedly in a mixture of ethanol and heptane. The resulting precipitate was dispersed in ethanol and was mixed with SiO₂:Pr³⁺ sol by stirring vigorously at room temperature until a gel formed. The gel was dried at room temperature, was ground and annealed in air at 600 °C for 2 h. SiO₂:Pr³⁺ and ZnO-SiO₂:Pr³⁺ samples were prepared with different concentrations of ZnO QDs (5–25 mol%) and Pr³⁺ (0.01–0.25 mol%). The samples were characterized by X-ray diffraction, UV-vis, CL spectroscopy and X-ray photoelectron spectroscopy (XPS). All the data were collected at room temperature.

3. Results and discussion

Fig. 1 shows the XRD patterns of the dried ZnO QDs and standard micron sized ZnO powders. The ZnO QDs consist of broadened diffraction peaks resembling those of the standard micron sized ZnO and they are consistent with the wurtzite structure of ZnO (JCPDS Card no 80-0075). The average particle size of the ZnO QDs estimated using the Scherrer equation was ~4 nm in diameter. The inset shows the XRD patterns of SiO₂:Pr³⁺ and ZnO-SiO₂:Pr³⁺ powders, all annealed at 600 °C for 2 h. The broad band from the amorphous SiO₂ was observed at $2\theta \sim 20$ –25°. There were no diffractions from either the ZnO QDs or the Pr³⁺ ions probably due to their relatively low concentrations.

* Corresponding author. Tel.: +27 51 401 2193; fax: +27 51 401 3507.
E-mail address: ntwaeab@ufs.ac.za (O.M. Ntwaeaborwa).

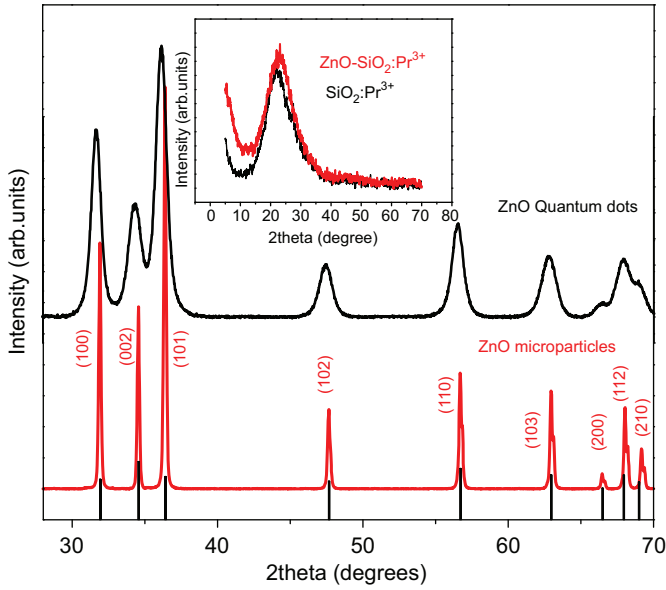


Fig. 1. X-ray diffraction pattern of ZnO microparticles, ZnO quantum dots and standard ZnO data (JCPDS Card no. 80-0075). The inset shows XRD patterns of $\text{SiO}_2:\text{Pr}^{3+}$ and $\text{ZnO-SiO}_2:\text{Pr}^{3+}$ powder phosphors.

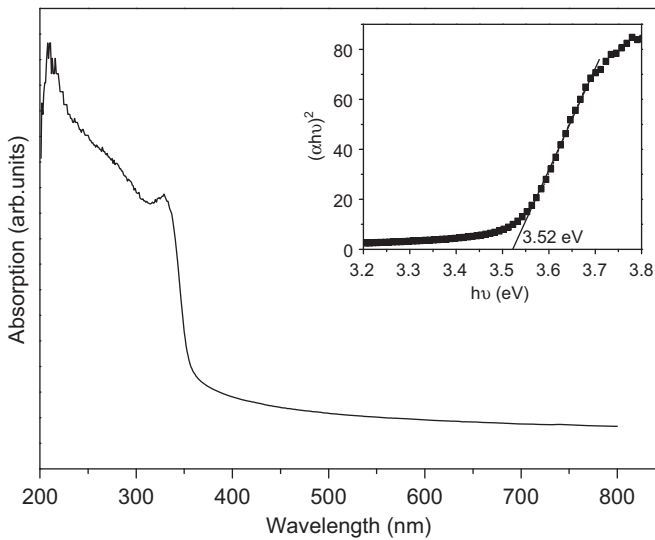


Fig. 2. UV-vis absorption spectrum of ZnO quantum dots. The plot of $(\alpha hv)^2$ vs photon energy ($h\nu$) is shown in the inset.

The UV-vis absorption spectrum of the ZnO QDs is shown in Fig. 2. The optical absorption peak, which can be ascribed to the excitonic transition [9] was observed at ~ 328 nm. The inset shows the plot of $(\alpha hv)^2$ versus $h\nu$, where α is the absorption coefficient and $h\nu$ is the photon energy. The optical band gap of ZnO QDs was estimated using the Tauc's relation [10]. By extrapolating the linear region of the plot to $(\alpha hv)^2=0$ axis, the direct band gap energy value was found to be 3.52 eV. This value is larger than the band gap energy of bulk ZnO and this can be attributed to the quantum confinement effects [11]. Assuming that the particles are spherical, the average particle size of the ZnO QDs was estimated using the following equation [12]:

$$E(r) \simeq E_g + \frac{\hbar^2 \pi^2}{2r^2} \left[\frac{1}{m_e} + \frac{1}{m_h} \right] - \frac{1.8e^2}{\epsilon r} \quad (1)$$

where $E(r)$ =quantum dots band gap as a function of particle radius r , E_g =bulk band gap, m_e =effective mass of electrons, m_h =effective mass of holes, e =elementary charge of an electron

and ϵ =dielectric constant. The following values were used to estimate the average particle radius: $E(r)=3.52$ eV (ZnO), $E_g=3.29$ eV (ZnO), $\hbar=1.054 \times 10^{-34}$ J.s, $m_e=0.24m_0$ [12] (m_0 is the free electron mass= 9.11×10^{-31} kg), $m_h=0.45m_0$, ϵ (ZnO)=8.6 and the average particle diameter of ~ 6 nm was obtained and was comparable to the XRD results. Fig. 3 shows the CL spectra of the undoped SiO_2 and $\text{SiO}_2:\text{Pr}^{3+}$ with different Pr^{3+} concentrations (0.01–0.25 mol%). Defects emission from SiO_2 was observed at 470 nm and it was quenched when Pr^{3+} was incorporated. Multiple emission peaks located at approximately 495 nm, 614 nm (main emission), 724 nm and 970 nm, which are attributed to ${}^3\text{P}_0-{}^3\text{H}_4$, ${}^3\text{P}_0-{}^3\text{H}_6$, ${}^3\text{P}_0-{}^3\text{F}_3$ and ${}^1\text{D}_2-{}^3\text{F}_4$, respectively [13–16], were observed from $\text{SiO}_2:\text{Pr}^{3+}$. The CL intensity increased with Pr^{3+} concentration (0.01–0.2 mol%), and the maximum intensity was observed at 0.2 mol% and the intensity decreased when the concentration was increased to 0.25 mol% probably due to the concentration quenching effects. The concentration quenching effects are due to cross relaxation and energy migration as a result of clustering of activator ions beyond a certain concentration [17]. The CL emission spectra of $\text{ZnO-SiO}_2:\text{Pr}^{3+}$ powders with different concentrations (15–25 mol%) of ZnO QDs are shown in Fig. 4 when the concentration

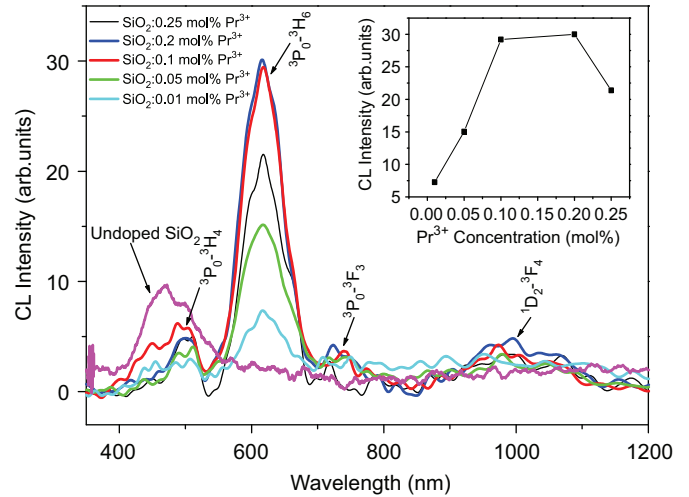


Fig. 3. CL spectra of SiO_2 and $\text{SiO}_2:\text{Pr}^{3+}$ with different concentrations of Pr^{3+} ions. The inset shows the maximum CL intensity vs the Pr^{3+} ions concentration.

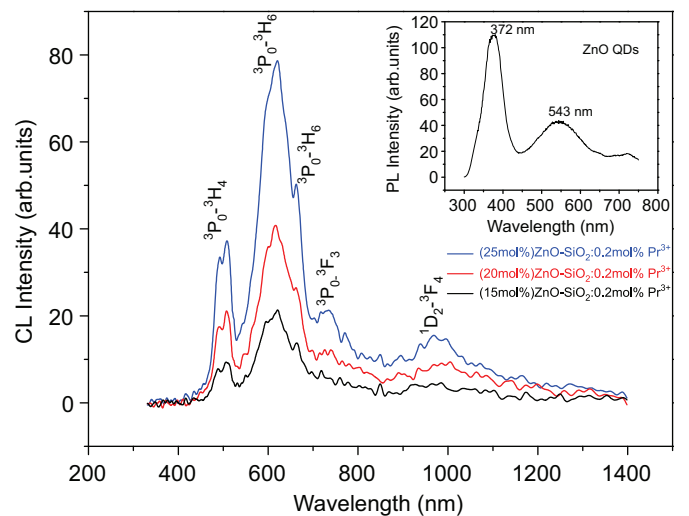


Fig. 4. $\text{ZnO-SiO}_2:\text{Pr}^{3+}$ with different concentration of ZnO QDs. The inset is the fluorescence spectra of ZnO quantum dots.

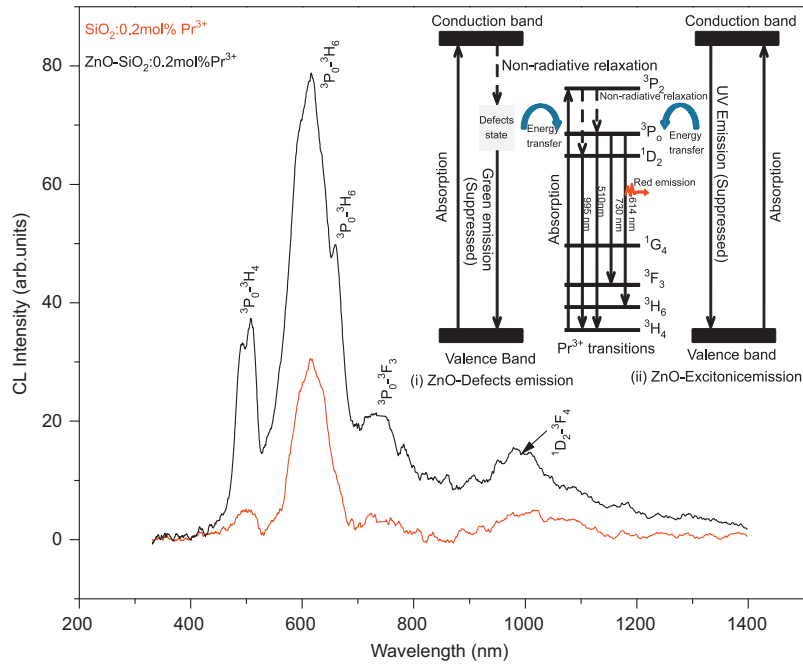


Fig. 5. CL spectra of SiO₂:0.2 mol%Pr³⁺ and 25 mol%ZnO-SiO₂:0.2 mol%Pr³⁺. The inset is the simplified energy diagrams of ZnO and Pr³⁺ to explain energy transfer.

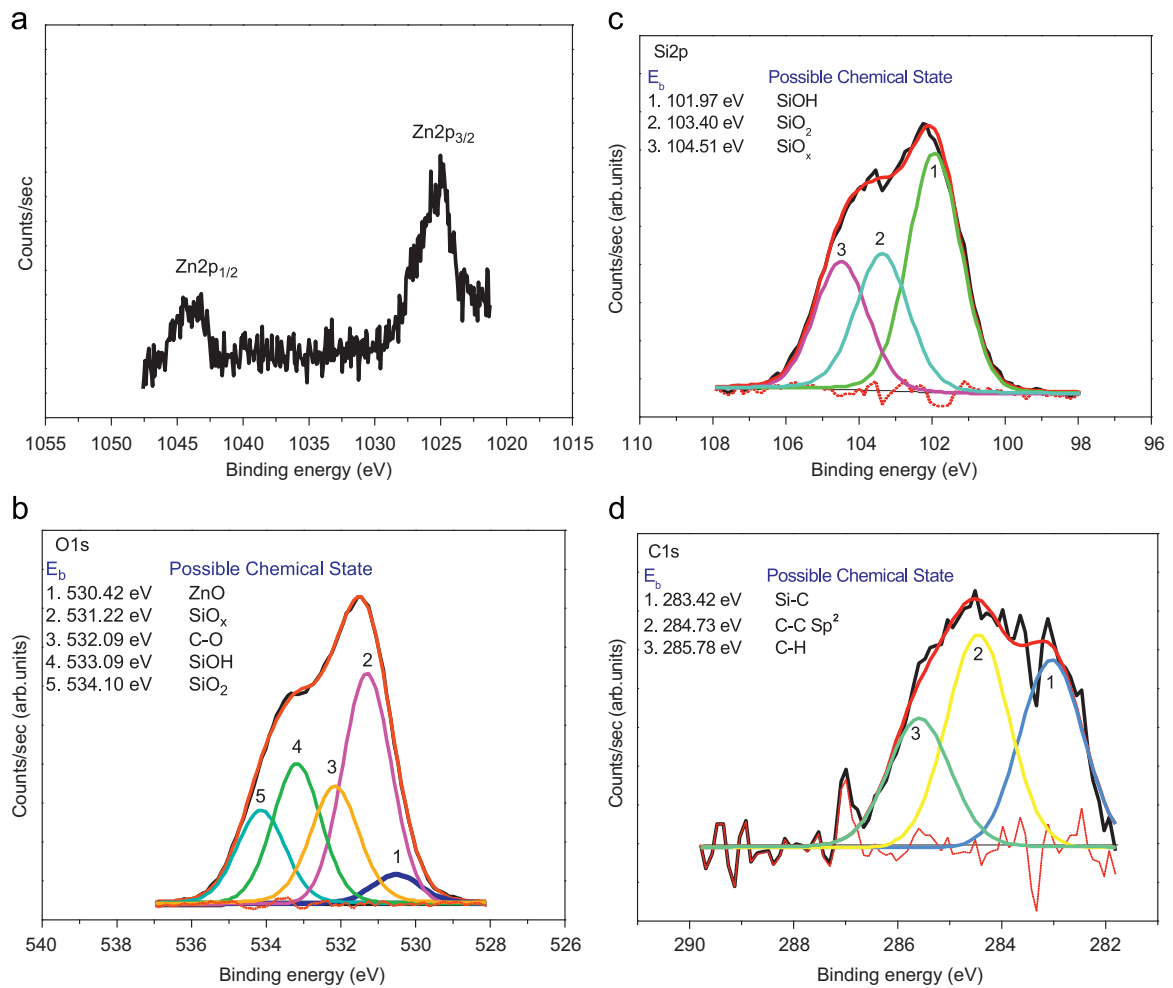


Fig. 6. High resolution X-ray photoelectron spectra of (a) Zn2p, (b) O1s, (c) Si2p and (d) C1s.

of Pr^{3+} was fixed at 0.2 mol%. The maximum CL intensity was observed at 25 mol% of ZnO. The inset shows the fluorescence spectrum of ZnO QD with dual emissions at ~ 372 and 543 nm. This spectrum was recorded when ZnO powder was excited at 250 nm with a monochromatized xenon lamp, and it is consistent with the CL spectrum of ZnO QDs reported by Ma et al. [18]. Although we could not measure the CL spectra from ZnO due to charging, it is well known that the ZnO QD usually displays dual emissions in the UV and visible regions irrespective of the type of excitation (i.e. UV photons or electrons). The fact that the ZnO emission was suppressed in $\text{ZnO-SiO}_2:\text{Pr}^{3+}$ with a subsequent increase in the red emission of Pr^{3+} suggests that energy was transferred from ZnO to Pr^{3+} . The maximum CL intensities as shown in Figs. 3 and 4 are compared in Fig. 5. It shows that the CL intensity was increased by about a factor of 3 when the ZnO QDs were incorporated. The possible mechanism of energy transfer from ZnO to Pr^{3+} is illustrated in the inset of Fig. 6. It is speculated that both the UV (~ 372 nm) and the defects (~ 543 nm) emissions contributed to the energy transfer process given that the red emission from Pr^{3+} emanates from the states lying lower than both the UV and the defects emissions from the ZnO QDs. According to the illustration, an exciton created in the ZnO band gap can transfer energy non-radiatively to Pr^{3+} states with a rate faster than the hole trapping and recombination with electrons by defect states or energy can also be transferred by defect states following hole trapping and recombination with electrons. The energy was most probably transferred by a phonon mediated process via internal photoemission from ZnO to the $^3\text{P}_0$ state of Pr^{3+} . The reader is referred to the literature cited in Refs.[3,5,19,20] for further reading on energy transfer from ZnO to rare-earth ions.

Fig. 6(a–d) depicts the high resolution XPS spectra of Zn2p, O1s, Si2p and C1s, respectively. The high resolution spectra of Zn2p in Fig. 6(a), show two distinct Zn2p_{3/2} and Zn2p_{1/2} states at 1022 ± 0.1 eV and 1043.9 ± 0.1 eV, respectively. The O1s peak in Fig. 6(b) was deconvoluted into five peaks at 530.42 eV, 531.22 eV and 532.09 eV, 533.09 eV and 534.10 eV due to possible chemical states presented in the figure. The high resolution peak of Si2p was deconvoluted into three peaks at 101.97 eV, 103.40 eV and 104 eV as shown in Fig. 6(c), which can be attributed to the contribution from silicon in SiOH, SiO₂ and SiO_x, respectively. The C1s was deconvoluted into three peaks at 283.42 eV, 284.73 eV and 285.78 eV due to C in Si–C, C–C sp² and C–H, respectively, which originates from the sample preparation and manipulation. These data are in agreement with the data reported in Refs. [21–25].

4. Conclusion

Red-emitting $\text{SiO}_2:\text{Pr}^{3+}$ and $\text{ZnO-SiO}_2:\text{Pr}^{3+}$ powder phosphors were successfully synthesized by the sol-gel method. The Pr^{3+}

ions' maximum emission was observed at 0.2 mol% doping concentration. It was demonstrated that the CL intensity of Pr^{3+} in an amorphous SiO₂ host was increased by the energy transfer from the ZnO QDs to Pr^{3+} with the maximum transfer observed when 25 mol% of ZnO was incorporated. The XPS analysis showed electronic states and related chemical species present in the samples.

Acknowledgments

The authors would like to thank the South African National Research Foundation (NRF) and The University of the Free State for financial support.

References

- [1] A.B. Djuricic, A.M.C. Ng, X.Y. Chen, Prog. Quantum Electron 34 (2010) 191.
- [2] Y. Yu, Y. Wang, D. Chen, P. Huang, E. Ma, F. Bao, Nanotechnology 19 (2008) 055711-1.
- [3] O.M. Ntwaeaborwa, P.H. Holloway, Nanotechnology 16 (2005) 865.
- [4] M.S. Dhlamini, O.M. Ntwaeaborwa, H.C. Swart, Ngaruiya, K.T. Hillie, Physica B 404 (2009) 4406.
- [5] J.S. Bang, H. Yang, P.H. Holloway, J. Phys. Chem 123 (2005) 084709-1.
- [6] A.A. Ismail, M. Abboudi, P. Holloway, H. El-Shall, Mater. Res. Bull. 42 (2007) 137.
- [7] G.H. Mhlongo, O.M. Ntwaeaborwa, M.S. Dhlamini, H.C. Swart, K.T. Hillie, J. Mater. Sci. 45 (2010) 5228.
- [8] Ke-Li Zhang, Jian-He Hong, Chang-Jie Cong, Zhi-Guo Zhang, J. Phys. Chem. Solids 68 (2007) 1359.
- [9] D. Bera, L. Quian, S. Sabui, S. Santra, P.H. Holloway, Opt. Mater. 30 (2008) 1233.
- [10] G.P. Joshi, N.S. Saxena, R. Mangal, A. Mishra, T.P. Sharma, Bull. Mater. Sci. 26 (2003) 387.
- [11] B. Bhattacharjee, D. Ganguli, S. Chadhuri, A.K. Pal, Thin Solid Films 422 (2002) 98.
- [12] L. Brus, J. Phys. Chem. 90 (1986) 2555.
- [13] W. Strek, J. Legendziewicz, E. Lukowiak, K. Maruszewski, J. Sokolnicki, A.A. Boiko, M. Borzechowska, Spectrochim. Acta A 54 (1998) 2215.
- [14] C.M. Donega, A. Meijerink, G. Blasse, J. Phys. Chem. Solids 56 (5) (1995) 673.
- [15] P. Boutinaud, E. Pinel, M. Dubois, A.P. Vink, R. Mahiou, J. Lumin. 111 (2005) 69.
- [16] P.N. Zhmnrin, N.V. Znamemskii, T.G. Yukina, Yu.V. Malyukin, Phys. Status Solidi 224 (2007) 3325.
- [17] C. Jia, E. Xie, A. Peng, R. Jiang, F. Ye, H. Lin, T. Xu, Thin Solid Films 496 (2006) 555.
- [18] Q. Ma, T.E. Saraswati, A. Ogini, M. Nagatsu, Appl. Phys. Lett. 98 (2011) 051903-1.
- [19] M.S. Dhlamini, G.H. Mhlongo, H.C. Swart, K.T. Hillie, J. Lumin. 131 (2011) 790.
- [20] M.S. Dhlamini, O.M. Ntwaeaborwa, H.C. Swart, J.M. Ngaruiya, K.T. Hillie, Physica B 33 (2010) 79.
- [21] A.G. Joshi, S. Sahai, N. Gandhi, Y.G.D. Krishna, D. Haranath, Appl. Phys. Lett. 96 (2010) 123102-1.
- [22] L. Fernandez, N. Garro, J.E. Haskouri, M. Perez-Cabero, J. Avarez-Rodriguez, J. Latorre, C. Guillem, A. Beltran, D. Beltran, P. Amoros, Nanotechnology 19 (2008) 225603-1.
- [23] R. Wahab, S.G. Ansari, H.K. Seo, Y.S. Kim, E.K. Suh, H.S. Shin, Solid State Sci. 11 (2009) 439.
- [24] J.F. Moulder, W.F. Stickle, P.E. Sobol, K.D. Bomben, Handbook of X-ray Photoelectron Spectroscopy, Perkin-Elmer Corporation, 1992.
- [25] S.S. Pitale, I.M. Nagpure, V. Kumar, O.M. Ntwaeaborwa, J.J. Terblans, H.C. Swart, Mater. Res. Bull. 46 (7) (2011) 987.